Vol. 03, No. 2, December 2024, pp. 69-78
p-ISSN: 2963-8577
e-ISSN: 2964-3511
DOI: 10.57102/jescee.v3i2.82

QUANTIFYING MEASUREMENT UNCERTAINTY USING WEIGHTED LEAST SQUARES FOR FORCE MEASUREMENT IN BIOMIMETIC ROBOT DEVELOPMENT

Muhammad Farhan[1], Arie Sukma Jaya[1*]
[1]Department of Mechanical Engineering, Faculty of Industrial Technology, Universitas Pertamina

Abstract
Robotics is one area where biomimetics, a field devoted to mimicking natural systems to address difficult human problems, has made great strides. Precise force measurement and analysis are vital to this field because they are necessary to reproduce and comprehend natural phenomena. This study addresses the challenge of accurate force measurement by developing a load cell-based device. It specifically assesses the impact of the taring process on measurement accuracy. The Weighted Least Squares (WLS) method is employed to thoroughly quantify the uncertainty of the device, ensuring reliability. The findings suggest that the single-input taring process contributes to variations in standard deviation, with accuracy peaking near the tared value and decreasing as the mass deviates from it. The linear calibration equation derived from WLS showed minimal variation in estimated mass values, with uncertainties $u_a = 2 \times 10^{-6}$ and $u_b = 8 \times 10^{-4}$. However, the expanded uncertainty increased with the input mass, largely due to the inherent uncertainty of the mass balance. Despite this, the hysteresis of the system was negligible, and its sensitivity of 0.01 N/g made it suitable for detecting small force fluctuations in biomimetic models. The study concludes that while the relative value of the maximum combined uncertainty, U_{Lc} = ±0.2% FSS, exceeds the reference specifications of the load cell, it remains adequate for applications requiring moderate precision. Future research will reduce mass balance uncertainty and consider environmental factors, thereby improving system effectiveness in biomimetic research.

Keywords:
force measurement; uncertainty; Weighted Least Squares (WLS); biomimetics; robotics

Article History:
Received: August 10th, 2024
Revised: November 29th, 2024
Accepted: December 11th, 2024
Published: December 13th, 2024

Corresponding Author:
Arie Sukma Jaya
Department of Mechanical Engineering, Universitas Pertamina, Indonesia
Email:
arie.sj@universitaspertamina.ac.id

1. Introduction

Biomimetics has recently emerged as a dynamic field of study that seeks to solve complex human problems by emulating natural models, systems, and elements [1,2,3]. Observing and mimicking natural processes has allowed this multidisciplinary approach to be applied to a variety of domains, including robotics, materials science, and medical devices. The essence of biomimetics is its ability to obtain inspiration from the efficiency and adaptability of biological systems [4,5,6]. However, the successful implementation of these nature-inspired solutions frequently relies on precise measurement and analysis, particularly in the context of forces and interactions, which are critical for understanding and replicating natural phenomena. Precision force measurements are required for more than just data collection; they are critical for validating theoretical models and ensuring experiment reproducibility [7,8,9,10]. As a result, developing tools that can precisely measure these forces is a critical challenge in the advancement of biomimetics.

High precision in force measurement instruments is required due to the inherent uncertainties that can arise during experiments [11,12,13]. These uncertainties can come from a variety of sources, including environmental factors, instrument calibration, and the intrinsic properties of the materials under investigation. Inaccurate force

measurements can cause significant errors in data interpretation, potentially leading to false conclusions about the behavior of the biomimetic systems under investigation. Thus, reducing these uncertainties is critical for achieving reliable and reproducible results. To address these challenges, researchers must improve the sensitivity and accuracy of their measurement tools and thoroughly quantify and account for any uncertainties in their data.

This study aims to develop a force measurement device using a simple yet highly precise load cell. By optimizing its design and calibration, the research seeks to achieve exceptional accuracy in force measurements, making the device ideal for delicate and detailed biomimetic studies. The simplicity of the device is intentionally designed to ensure accessibility and ease of use, without sacrificing measurement accuracy or reliability. While most available load cells are compatible with microcontroller boards via ADC modules that enable taring—a common practice that sets the baseline for measurements—the accuracy of this process has not been thoroughly assessed. This study addresses this gap by quantifying the uncertainty in tared load cell measurement systems. To quantify the uncertainty associated with the developed force measurement device, this study employs the Weighted Least Square (WLS) method [14,15,16]. The WLS method is a statistical approach that accounts for varying levels of uncertainty in different measurements, providing a more accurate estimation of the parameters being studied. By applying WLS, the study aims to identify and minimize the sources of uncertainty in the measurements, thus enhancing the overall reliability of the device. This approach not only improves the precision of the measurements but also provides a robust framework for assessing the quality of the data obtained. The use of WLS is particularly advantageous in biomimetic research, where the forces involved can be extremely small and sensitive to a wide range of factors. The ultimate goal of this research is to develop a reliable force measurement system for biomimetic studies, with a focus on rigorously quantifying its uncertainty. The uncertainty calculated using the WLS method will be compared with the initial load cell specifications to validate the performance of the device. Additionally, the developed setup will be tested in preliminary continuous force measurements of a biomimetic model. The outcomes of this study are expected to significantly advance the field of biomimetics, providing researchers with new tools and methodologies to explore the intricate interactions within natural systems.

2. Method

A. Calibration and uncertainty quantification

The current study utilizes the Weighted Least Square (WLS) method to approximate linear equations and directly calculate the uncertainty of measured parameters. It links the actual mass of the load with the output reading of the measured mass through the linear Equation (1):

$$m_C = b + a\, x_c \tag{1}$$

where m_c is the actual mass of in grams, b is the intercept constant, a is the slope of the calibration curve, and x_c is the output reading of the measured mass in grams. The coefficient vector, C, is calculated using Equation (2) where X represents the average measured values, Y denotes the reference values, and superscript T indicates the transpose of the parameters.

$$(X^T.X).C = X^T.Y \tag{2}$$

$$X = \begin{bmatrix} x_{1,1} & x_{1,2} \\ \vdots & \vdots \\ x_{j,1} & x_{j,2} \end{bmatrix} \tag{3}$$

$$Y = \begin{bmatrix} \frac{m_{c,1}}{w_1} \\ \vdots \\ \frac{m_{c,j}}{w_j} \end{bmatrix} \tag{4}$$

$$w_j = \sigma_{x_i}^2 \tag{5}$$

$$Q = (X^T.X)^{-1} \tag{6}$$

In the Equation (3) X is a j x 2 matrix with elements $x_{j,1} = \frac{1}{w_j}$ and $x_{j,2} = \frac{x_i}{w_j}$, where x_i is the output reading of the measured mass using a bar load cell. The column vector Y in Equation (4) represents the weighted value of the input mass, determined by dividing the actual mass, m_c, by a weighting factor, w_j. The weighting factor, w_j, as defined in Equation (5) is derived from the variance of the output reading x_j. Equation (6) describes the Q matrix, where the diagonal elements represent the variance of the linear equation coefficients a and b, and the off-diagonal elements represent their covariance. Uncertainty is a parameter that indicates the distribution of a measured quantity [17,18,19]. In this study, two types of uncertainty are considered: type A and type B. Type A uncertainty is calculated through repeated direct measurements, while type B uncertainty is based on existing information, such as manufacturing specifications and reference data. The type A uncertainty of forces, based on calibration values, u_L, follows the law of uncertainty propagation in Equation (7):

$$u_L = \left(a^2 u_{mo}^2 + u_b^2 + m_o^2 u_a^2 + 2m_o Cov(b,a)\right)^{0.5} \quad (7)$$

where u_{mo} is the uncertainty due to changes in output mass readings, u_a and u_b are the uncertainties of the calibration curve equation coefficients (a and b), m_o is the load cell output mass reading, and $Cov(b,a)$ is the covariance of the calibration curve coefficients.

$$u_{mo}^2 = u_m^2 + u_R^2 \quad (8)$$

$$u_m = \frac{s_m}{\sqrt{n}} \quad (9)$$

$$u_R = \frac{r}{\sqrt{3}} \quad (10)$$

Equation (8), (9), and (10) describe the uncertainty components of the mass output reading, where u_m is the standard deviation of the average measurement value, s_m is the standard deviation of repeated measurements, n is the number of repeated measurements, u_R is the uncertainty of the resolution of the data acquisition, and r is the smallest resolution value of the mass output reading. In this study, n is 10 while r is 0.1 gr.

The combined expanded uncertainty with a 95.45% confidence level for the load cell is:

$$u_{Lc} = \sqrt{(u_L^2 + u_{Dm}^2)} \quad (11)$$
$$U_{Lc} = k \times u_{Lc} \quad (12)$$

where u_L is the calibration uncertainty from Equation (7), u_{Dm} is the mass uncertainty of the mass balance (0.5%), and k is the coverage factor (value of 2). The combined uncertainty, u_{Lc}, is then determined with Equation (11). The expanded combined uncertainty, U_{Lc}, is calculated by using Equation (12) by multiply the combine uncertainty with the coverage factor. The uncertainty of the force calculation by using the load cell can be calculated by using:

$$u_F = U_{Lc} \times g \quad (13)$$
$$u_{Fr} = (u_F/F_R) \times 100\% \quad (14)$$

where u_F in Equation (13) is the force absolute uncertainty and u_{Fr} in Equation (14) is the relative uncertainty, g is the gravity acceleration of 9.81 m/s^2, and F_R is the calculated force during calibration.

B. Calibration setup and scheme

The calibration setup for the implementation of the Weighted Least Squares (WLS) method is depicted in Figure 1. It comprises a standing frame, a load cell, balance masses, a microcontroller board, and a computer as the processing unit. The standing frame measures 50 cm in length, 50 cm in width, and 60 cm in height. This setup is designed to measure the vertical force of a contraction-expansion mechanism in an underwater environment. The load cell used is a YZC-131 type, with its technical specifications listed in Table 1 [20]. The mass balance includes four 50g weights, five 100g weights, and one 200g weight. An Arduino Pro Mini serves as the microcontroller board, processing sensor data and executing programmed commands. It also facilitates communication with the computer via serial ports (UART), enabling the transfer of measured digital data and reception of commands. The HX711 module, a precision 24-bit analog-to-digital converter (ADC), is connected between the load cell and the microcontroller board, using a two-wire interface (Clock and Data).

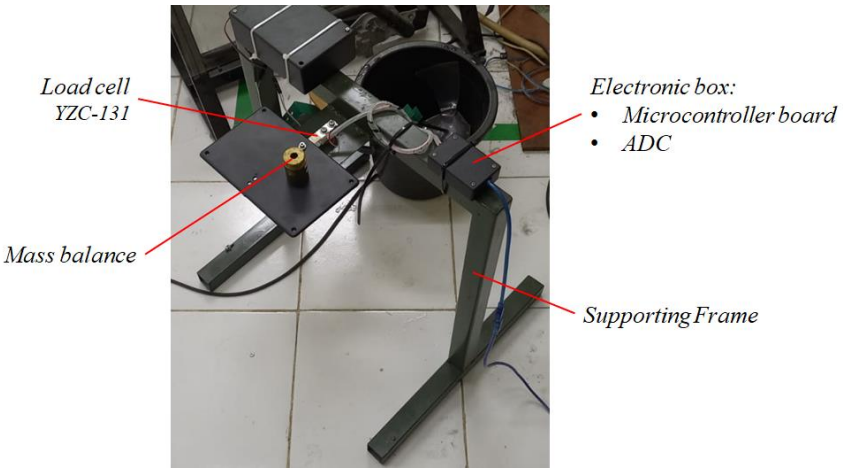

Figure 1. Calibration setup

Table 1. Specification of Load Cell Sensor YZC-131 (1 kg) [20]

Load Cell Type	Strain Gauge
Weighing Range	0 - 1 kg
Dimensions	75 mm × 12.7 mm × 12.7 mm
Precision	0.05%
Rated Output	1.0 ± 0.15 mV/V
Non-linearity	0.05% Full-Scale (FS)
Hysteresis	0.03% FS
Non-Repeatability	0.03% FS
Input Impedance	1000 ± 50 Ω
Output Impedance	1000 ± 50 Ω
Excitation Voltage	5 VDC

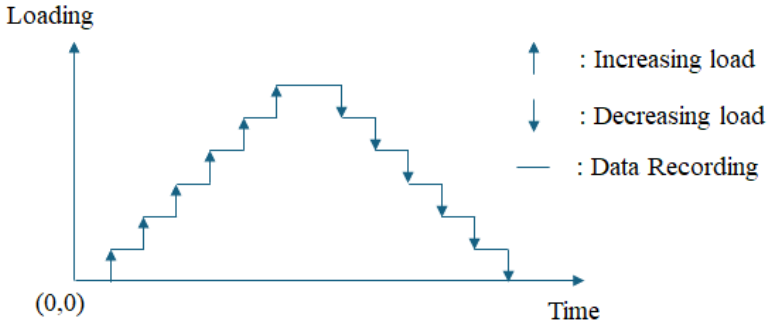

Figure 2. Calibration loading scheme

Figure 2 depicts a calibration loading scheme. It consists of three steps: increasing the load, decreasing the load, and recording the data. The sequence begins with no load (0,0), then adds a known 50 g load and measures the mass. This procedure is repeated with increasing loads until the maximum weight is attained. The load is then reduced in reverse order, with readings taken at each step. This procedure is repeated five times to ensure reliable data and high confidence in the validity of the results. Before mass calibration, the load cell was programmatically tared in accordance with the HX711 module specifications, which served as a pre-calibration step. This process produces the initial calibration factor, which is the ratio of the reading to the known weight. The pre-calibration was done with a known weight of 202.2 g, resulting in a reading of 218801 and a calibration factor of 1093.

3. Result and Discussion

Table 2 provides a detailed account of the output readings corresponding to the measured mass at various stages. The table includes data from eleven distinct stages where the load was incrementally increased and then decreased, referred to as the "Up" and "Down" loading stages. Each stage represents a specific load cycle, designed to evaluate the performance of the system under varying conditions. For each stage, the output reading is recorded, and the average value, along with the standard deviation, is calculated based on five repetitions of the loading cycles. These statistical measures, shown in the last two columns of the table, help assess the consistency and reliability of the measurement process. It is important to note that the system has already tared, ensuring that the input mass and output reading are expressed in the same unit of grams. The data reveals that the maximum standard deviation observed is 0.05 grams, a figure that predominantly appears during the initial and final stages of the loading process. This indicates that the precision of the system is slightly lower at the extremes of the loading range. The use of a single known input for the taring process may also contribute to this variability in standard deviation. The standard deviation appears to stabilize around 200g, reaching peak accuracy near 400g, before increasing again as the mass deviates further from the tared value.

Table 2. Output reading of the measured mass

No	Mass (gr)	First Loading (gr)		Second Loading (gr)		Third Loading (gr)		Fourth Loading (gr)		Fifth Loading (gr)		Average (gr)	Standard deviation (gr)
		Up	Down	Up	Down	Up	Down	Up	Down	Up	Down		
1	0	0.0	0.2	0.2	0.2	0.2	0.1	0.1	0.1	0.2	0.2	0.1	0.05
2	50.6	50.2	50.3	50.3	50.3	50.3	50.2	50.3	50.3	50.4	50.4	50.3	0.05
3	100.6	100.4	100.5	100.5	100.5	100.5	100.4	100.4	100.4	100.5	100.5	100.4	0.04
4	150.6	150.4	150.5	150.5	150.5	150.5	150.4	150.4	150.5	150.5	150.5	150.4	0.04
5	200.8	200.4	200.5	200.4	200.5	200.5	200.4	200.5	200.5	200.5	200.5	200.5	0.04
6	300.8	300.7	300.7	300.7	300.8	300.7	300.7	300.7	300.8	300.7	300.7	300.7	0.03
7	400.8	400.8	400.7	400.8	400.8	400.8	400.7	400.8	400.8	400.8	400.7	400.8	0.02
8	501	501.0	501.0	501.0	501.0	501.1	501.0	501.0	501.0	501.0	501.0	501.0	0.03
9	601	601.0	601.0	601.1	601.1	601.1	601.0	601.0	601.0	601.0	601.0	601.0	0.03
10	701.4	701.3	701.3	701.2	701.2	701.3	701.2	701.2	701.2	701.2	701.2	701.2	0.05
11	901.6	901.6	901.6	901.6	901.6	901.7	901.7	901.5	901.5	901.6	901.6	901.6	0.05

Table 3. Linear model properties

w	*X*		*Y*
0.003	336.2	44.5	0.0
0.002	434.4	21851.8	21981.7
0.001	760.2	76358.6	76474.8
0.001	793.4	119366.2	119485.6
0.002	665.8	133474.8	133699.0
0.001	914.3	274972.6	275032.8
0.001	1655.9	663613.4	663672.6
0.001	1053.4	527769.8	527750.7
0.001	1370.5	823746.2	823687.8
0.002	467.9	328093.3	328176.0
0.002	432.1	389561.4	389556.5

Table 3 illustrates the components of the linear regression model, specifically the matrix *X*, vector *Y*, and weight *w*, as derived from Equations (3), (4), and (5). The matrix *X* represents the input variables, the vector *Y* corresponds to the observed outcomes, and the weight *w* is assigned to each observation to account for its uncertainty. In this context, the weight reflects the level of confidence in each measurement, where smaller variances indicate more reliable (or certain) observations, and thus, receive smaller weights. Conversely, observations with larger variances, which are less reliable (or uncertain), are assigned larger weights. This weighting process is crucial for the Weighted Least Squares (WLS) estimation method used in this study, as it ensures that observations with higher uncertainty have a proportionately smaller influence on the final model.

Table 4 presents the key properties of the calibration curve derived from the experimental data. The intercept and slope of the calibration curve are obtained using Equation (2), while the uncertainties and covariance associated with these properties are calculated through Equation (6). These parameters define the load cell calibration equation, which is expressed as $m_C = 0.193 + 1.000\, x_c$ in units of grams, as shown in Equation (1). This equation provides a mathematical relationship between the measured output and the actual mass, allowing for accurate calibration of the load cell. The uncertainties associated with the coefficients of the linear model in the current calibration process are notably small, indicating a high degree of confidence in the accuracy and reliability of the calibration results. This precision emphasizes the effectiveness of the calibration procedure, and the robustness of the model used in this study.

Table 4. Calibration curve properties

Intercept (*b*)	0.193
Slope (*a*)	1.000
u_a	2×10^{-6}
u_b	8×10^{-4}
cov(*a*,*b*)	-1×10^{-9}

Table 5. Expanded uncertainty of the measurement

No	Massa [gr]	Output reading, m_o [gr]	u_m [gr]	u_R [gr]	u_{mo} [gr]	u_L [gr]	u_{Dm} [gr]	u_{LC} [gr]	U_{LC} [gr]
1	0.0	0.1	0.02	0.06	0.06	0.06	0.0	0.1	0.1
2	50.6	50.3	0.02	0.06	0.06	0.06	0.3	0.3	0.5
3	100.6	100.4	0.02	0.06	0.06	0.06	0.3	0.3	0.5
4	150.6	150.4	0.02	0.06	0.06	0.06	0.3	0.3	0.5
5	200.8	200.5	0.02	0.06	0.06	0.06	0.3	0.3	0.5
6	300.8	300.7	0.01	0.06	0.06	0.06	0.5	0.5	1.0
7	400.8	400.8	0.01	0.06	0.06	0.06	0.5	0.5	1.0
8	501.0	501.0	0.01	0.06	0.06	0.06	0.5	0.5	1.0
9	601.0	601.0	0.01	0.06	0.06	0.06	0.5	0.5	1.0
10	701.4	701.2	0.02	0.06	0.06	0.06	0.5	0.5	1.0
11	901.6	901.6	0.02	0.06	0.06	0.06	1.0	1.0	2.0

Table 5 provides a comprehensive summary of the expanded uncertainty calculations involved in the calibration process. The uncertainty components listed in each column are determined through a series of calculations based on Equations (7) through (12). These calculations are essential in quantifying the various sources of uncertainty that contribute to the overall measurement error. The final column of the table presents the combined expanded uncertainty U_{Lc} at a confidence level of 95.45%. A notable trend in the data is that the combined expanded uncertainty increases with the increasing input mass. This trend may be primarily attributed to the characteristics of the mass balance used in the calibration process, where the uncertainty associated with the mass measurement tends to increase as the mass itself increases. This observation suggests that the mass balance currently employed in the calibration process might benefit from future improvements, specifically targeting a

reduction in its inherent uncertainty. Ensuring that the mass balance has a very small and stable uncertainty across a wide range of masses would enhance the accuracy and reliability of the calibration.

For applications involving the measurement of force, the input and output mass readings can be converted into force measurements by multiplying by the standard acceleration due to gravity. This conversion is crucial for contexts where force, rather than mass, is the primary quantity of interest. Figure 3 illustrates the relationship between the input calibration weight and the output estimated weight as derived from the linear calibration equation. The figure demonstrates a strong agreement between the calibration data points and the estimated line of best fit P_e. This close alignment indicates that the linear model provides an accurate representation of the calibration process. The figure also includes lines representing the uncertainty bounds P_{e+} and P_{e-}, which define the range of uncertainty associated with the output estimates. It is evident from the figure that the input calibration weights consistently fall within the bounds of the output uncertainty, affirming the reliability of the calibration. Additionally, three inset figures are provided to emphasize the observed increase in uncertainty with the increasing input weight. These insets offer a more detailed view of the relationship between input weight and uncertainty, highlighting the importance of accounting for this trend in the calibration process.

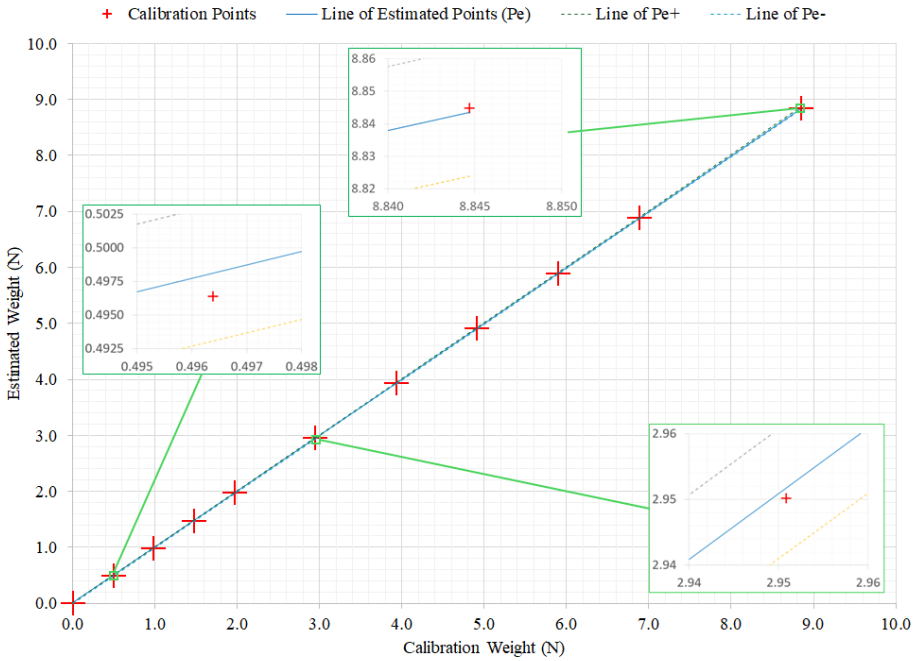

Figure 3. Calibration points and estimated curve by the model based on WLS and associated uncertainties (inset: Zoom view near the Calibration Weight of 0.496 N, 2.951 N, and 8.845 N)

The outcomes related to hysteresis, expanded uncertainty, and sensitivity of the force measurement systems are detailed in Table 6. The maximum observed hysteresis is notably small when expressed as a percentage of the Full-Scale Span (FSS) of the measurement system. This suggests that the hysteresis effect, which could potentially introduce errors into the measurements, is minimal and unlikely to significantly impact the overall accuracy of the system. However, the expanded uncertainty values exhibit a relatively higher percentage when compared to the FSS, especially in contrast to the specifications of the load cell provided in Table 1. This observation implies that the Weighted Least Squares (WLS) method employed in this study may capture a broader range of uncertainty sources, thereby offering a more realistic assessment of the performance of the measurement system. The increased uncertainty values could also serve to confirm earlier indications regarding the high uncertainty associated with the mass balance used in the current setup. This suggests that the contribution of the mass balance to the overall uncertainty is significant and should be carefully considered in future calibrations. The sensitivity of the force measurement systems, as reflected in Table 6, is relatively high, indicating that the system is highly responsive to

changes in the applied force. This high sensitivity is crucial for accurately detecting small variations in force, which is essential in precision measurement applications.

Table 6. The maximum characteristic of the force measurement system

Hysteresis (N)	Expanded Uncertainty (N)	Sensitivity
7×10^{-4} (0,008% FSS)	±0,02 (±0,2% FSS)	0.01 (N/gr)

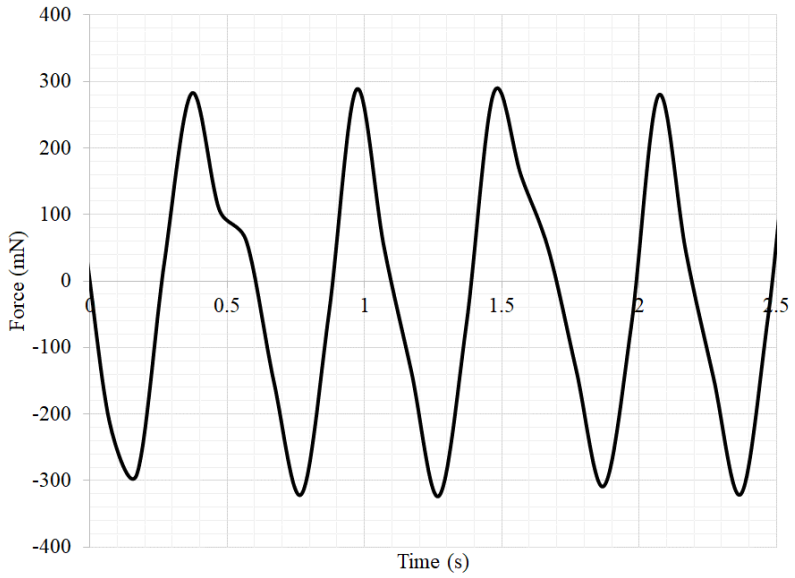

Figure 4. Continuous vertical force measurement using the present setup of calibrated systems

Figure 4 provides a sample of continuous vertical force measurements obtained using the current load cell configuration. The figure demonstrates that the present system is capable of capturing detailed and valuable information about the measured force. This capability is particularly important for applications that require precise force measurements over time. Additionally, the figure highlights specific aspects of the force measurement data that could be further analyzed for other applications. For instance, the ability of the system to measure expansion and compression forces makes it suitable for use in biomimetic models, where accurately replicating the mechanical properties of biological tissues is essential. The data captured by the system could provide insights into the behavior of such models under various force conditions, potentially leading to advancements in the design and evaluation of biomimetic systems.

4. Conclusion

This study has successfully conducted an uncertainty analysis of a measurement system using a load cell through a thorough calibration process. The Weighted Least Squares (WLS) method was employed to derive a linear calibration equation, applied to a repeated “Up” and “Down” loading scheme using a mass balance. The use of a single known input for the taring process may contribute to variations in standard deviation, with precision improving and reaching optimal performance near the tared mass. Beyond this point, the standard deviation increases as the mass diverges from the tared value, indicating the need for a more robust taring method to maintain accuracy across a wider range of measurements. The uncertainties associated with the linear curve coefficients, $u_a = 2 \times 10^{-6}$ and $u_b = 8 \times 10^{-4}$, contribute minimally to the variation in the estimated mass values, indicating the robustness of the calibration equation. However, the expanded uncertainty of the calibration process increases with the input mass, highlighting the significant impact of the inherent uncertainty of the mass balance on the overall uncertainty in the current setup. Despite this, the input calibration weight consistently falls within the estimated

weight range and its associated uncertainty. The hysteresis observed in the system, approximately 0.008% of the Full-Scale Span (FSS), is negligible and does not significantly affect the accuracy of the measurements. By accounting for uncertainties in both the measurement readings and the mass balance, the maximum combined uncertainty in this calibration process was determined to be ±0.02 N (±0.2% FSS). This value, though higher than the specified uncertainty of the load cell, is sufficient for applications requiring moderate precision. The sensitivity of the system, measured at 0.01 N/g, is adequate for detecting small fluctuations, making it particularly useful for force measurements in biomimetic models, where precise and responsive measurement systems are crucial. Future work could focus on further reducing the uncertainty of the input mass balance and incorporating environmental factors such as temperature and humidity into the uncertainty analysis. This improved setup would be highly valuable for more detailed investigations of forces in biomimetic models, potentially advancing the understanding of the field of biological systems and their mechanical properties.

Acknowledgment

The authors gratefully acknowledge the support and research facilities provided by Universitas Pertamina.

References

[1]. Y. Bar-Cohen and C. Breazeal, "Biologically Inspired Intelligent Robots," Biol. Inspired Intell. Robot., pp. 1–7, 2003, doi: 10.1117/3.2068093.

[2]. R. Wang, S. Wang, Y. Wang, L. Cheng, and M. Tan, "Development and Motion Control of Biomimetic Underwater Robots: A Survey," IEEE Trans. Syst. Man, Cybern. Syst., vol. 52, no. 2, pp. 833–844, Feb. 2022, doi: 10.1109/TSMC.2020.3004862.

[3]. K. Bu, X. Gong, C. Yu, and F. Xie, "Biomimetic Aquatic Robots Based on Fluid-Driven Actuators: A Review," *Journal of Marine Science and Engineering*, vol. 10, no. 6. MDPI, Jun. 01, 2022. doi: 10.3390/jmse10060735.

[4]. A. S. Jaya and M. W. Kartidjo, "Thrust and efficiency enhancement scheme of the fin propulsion of the biomimetic Autonomous Underwater Vehicle model in low-speed flow regime," Ocean Eng., vol. 243, Jan. 2022, doi: 10.1016/j.oceaneng.2021.110090.

[5]. A. S. Jaya, M. W. Kartidjo, B. W. Riyandwita, and Y. F. Buys, "Transition phase in the static thrust generation of the biomimetic fin with low oscillating frequency," Eng. Res. Express, vol. 5, no. 3, p. 035055, Sep. 2023, doi: 10.1088/2631-8695/acf275.

[6]. G. Li, G. Liu, D. Leng, X. Fang, G. Li, and W. Wang, "Underwater Undulating Propulsion Biomimetic Robots: A Review," Biomimetics, vol. 8, no. 3, 2023, doi: 10.3390/biomimetics8030318.

[7]. D. J. Callaghan, M. M. Mcgrath, and E. Coyle, "Force Measurement Methods in Telerobotic Surgery : Implications for End-Effector Manufacture," Proc. 25th Int. Manuf. Conf., pp. 389–398, 2008, doi: 10.21427/D7889V.

[8]. T. Shahid, D. Gouwanda, S. G. Nurzaman, and A. A. Gopalai, "Moving toward soft robotics: A decade review of the design of hand exoskeletons," Biomimetics, vol. 3, no. 3, 2018, doi: 10.3390/biomimetics3030017.

[9]. Q. Fu, H. C. Astley, and C. Li, "Snakes combine vertical and lateral bending to traverse uneven terrain," Bioinspir. Biomim., vol. 17, pp. 1–37, 2022, doi: 10.1088/1748-3190/ac59c5.

[10]. S. A. Brooks, J. D. Brooks, and M. A. Green, "Force measurements near a natural frequency of a measurement system using inverse filters," Meas. Sci. Technol., vol. 33, no. 2, 2022, doi: 10.1088/1361-6501/ac3943.

[11]. T. Bartel, "Uncertainty in NIST force measurements," J. Res. Natl. Inst. Stand. Technol., vol. 110, no. 6, pp. 589–603, 2005, doi: 10.6028/jres.110.084.

[12]. A. P. Singh, S. K. Ghoshal, H. Kumar, J. Yoon, and P. Yadav, "Development and Metrological Evaluation of a Force Transducer for Industrial Application," IEEE Access, vol. 9, pp. 33299–33312, 2021, doi: 10.1109/ACCESS.2021.3060746.

[13]. R. C. Hurley, "Stress and force measurement uncertainties in 3D granular materials," Powders Grains 2021 - 9th Int. Conf. Micromechanics Granul. Media, vol. 02009, pp. 1–4, 2021, doi: 10.1051/epjconf/202124902009.

[14]. M. Emmanouil and B. Vassilis, "Uncertainty and traceability in calibration by comparison," Meas. Sci. Technol., vol. 11, p. 771, 2000, [Online]. Available: http://stacks.iop.org/0957-0233/11/i=6/a=321

[15]. J. L. Ferreira *et al.*, "Application of weighted least squares to calibrate a digital system for measuring the respiratory pressures," BIODEVICES 2008 - Proc. 1st Int. Conf. Biomed. Electron. Devices, vol. 1, no. figure 1, pp. 220–223, 2008.
[16]. A. S. Jaya, M. W. Kartidjo, L. R. Zuhal, and I. S. Brodjonegoro, "Evaluation of force and torque measurement uncertainties of the three-component dynamometer of the biomimetic fin propulsion system," pp. 185–190, 2018.
[17]. L. Maybank, A. Knott, and D. Elkington, "Guide to the Uncertainty of Force Measurement," no. April, 1999.
[18]. J. C. F. G. I. Metrology, "Evaluation of measurement data — Guide to the expression of uncertainty in measurement," Int. Organ. Stand. Geneva ISBN, vol. 50, no. September, p. 134, 2008, [Online]. Available: http://www.bipm.org/en/publications/guides/gum.html
[19]. Euromet cg-4, "Uncertainty of Force Measurements Calibration Guide Version 2.0," 2011.
[20]. "YZC-131A Load Cells." [Online]. Available: https://www.electronicoscaldas.com/datasheet/YZC-131A.pdf

Biographies of Authors

Muhammad Farhan graduated in 2023 with a Sarjana Teknik degree from the Department of Mechanical Engineering at Universitas Pertamina. He is currently employed as an engineer at a private company in Jakarta.

Arie Sukma Jaya is a lecturer in the Department of Mechanical Engineering at the Faculty of Industrial Technology, Universitas Pertamina. His research interests include biomimetic robots and unmanned vehicles.